

## Design and Simulation of Dc/Dc Boost Converter

Aurobinda Prasad Panigrahy, Thakur Prasad Sahoo , Trupti Rath ,  
 Ansuman Rath , Srikanta Kumar Dash

*Department of Electrical and Electronics Engineering, , Gandhi Institute For Technology (GIFT), Bhubaneswar*

**Abstract:** *This paper presents a design and simulation of DC/DC boost converter. This system has a nonlinear dynamic behavior, as it work in switch-mode. Moreover, it is exposed to significant variations which may take this system away from nominal conditions, due to changes on the load or on the line voltage at the input. The input usually is obtained by PV array and therefore the design and simulation in this paper covers*

### I. INTRODUCTION

The DC/DC converters are widely used in regulated switch mode DC power supplies. The input of these converters is an unregulated DC voltage, which is obtained by PV array and therefore it will be fluctuated due to changes in radiation and temperature. In these converters the average DC output voltage must be controlled to be equated to the desired value although the input voltage is changing. From the energy point of view, output voltage regulation in the DC/DC converter is achieved by constantly adjusting the amount of energy absorbed from the source and that injected into the load, which is in turn controlled by the relative durations of the absorption and injection intervals. These two basic processes of energy absorption and injection constitute a switching cycle. Intuitively speaking, if the energy storage capacity of the converter is too small or the switching period is relatively too long, then the converter would have transmitted all the stored energy to the load before the next cycle begins. This introduces an idling period immediately following the injection interval, during which the converter is not performing any specific task [1,2,3]. The converter can therefore operate in two different modes depending upon its energy storage capacity and the relative length of the switching period. These two modes are known as the discontinuous conduction and continuous modes.

Graphically model of the boost converter is shown in Fig. 1. The full details of the boost converter topology have been already discussed in [4,5,6]. The DC/DC boost converter only needs four external components: Inductor, Electronic switch, Diode and output capacitor. The converter can therefore operate in the two different modes depending on its energy storage capacity and the relative length of the switching period. These two operating modes are known as the discontinuous conduction mode, DCM, and continuous conduction mode, CCM, corresponding to the cases with and without an idling interval respectively [6,7].

### II. METHODOLOGY

#### 2-1 Conversion modes

The DC/DC converter has two modes, a Continuous Conduction Mode, CCM for efficient power conversion and Discontinuous Conduction Mode DCM for low power or stand-by operation,

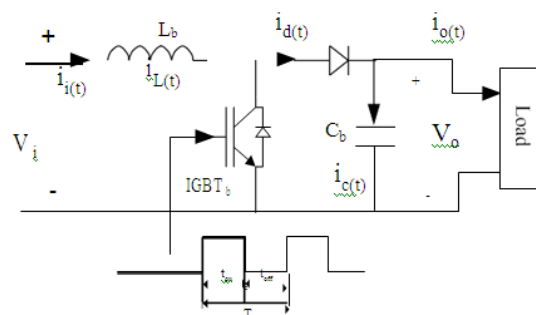


Fig. 1 Circuit Schematic of Step-up DC/DC Converter [8]

#### 2-1-1 Continuous Conduction Mode

Mode 1 ( $0 < t \leq t_{on}$ )

Mode 1 begins when IGBT's is switched on at  $t=0$  and terminates at  $t=t_{on}$ . The equivalent circuit for the mode 1 is shown in Fig. 2a. The inductor current  $i_L(t)$  greater than zero and ramp up linearly. The inductor voltage is  $V_i$ .

Mode 2 ( $t_{on} < t \leq T_s$ )

Mode 2 begins when IGBT's is switched off at  $t=t_{on}$  and terminates at  $t=T_s$ . The equivalent circuit for the mode 2 is shown in Fig. 2b. The inductor current decrease until the IGBT's is turned on again during the next cycle. The voltage across the inductor in this period is  $V_i-V_o$ . Since in steady state time integral of the inductor voltage over one time period must be zero.

$$V_i t_{on} + (V_i - V_o) t_{off} = 0 \quad [4,6] \quad (1)$$

Where;

- $V_i$  : The input voltage, V.
- $V_o$  : The average output voltage, V.
- $t_{on}$  : The switching on of the IGBT's, s
- $t_{off}$  : The switching off of the IGBT's, s

Dividing both sides by  $T_s$  and rearranging items yield

$$\frac{V_o}{V_i} = \frac{t_{on}}{T_s} = \frac{1}{1-D} \quad [4,6] \quad (2)$$

Where;

- $T_s$  : The switching period, s.
- $D$  : The duty cycle.

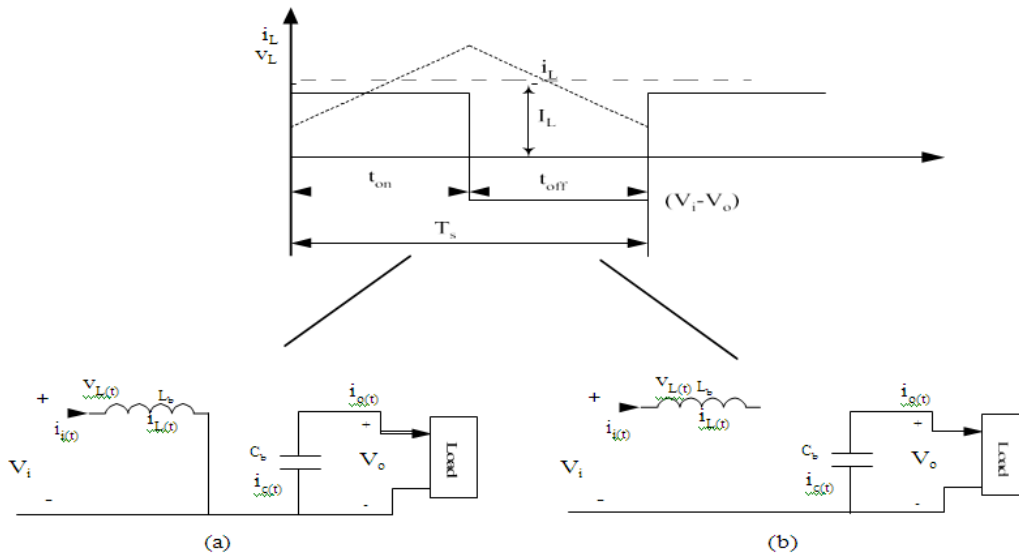


Fig. 2 Equivalent Circuit for boost Converter in CCM [4,6]

(a) Mode 1 ( $0 < t \leq t_{on}$ )

(b) Mode 2 ( $t_{on} < t \leq T_s$ )

Thus,  $V_o$  is inversely proportional to  $(1-D)$ . it obvious that the duty cycle,  $D$ , can not be equal to 1 otherwise there would be no energy transfer to the output. assuming a lossless circuit,  $P_i=P_o$ , then

$$I_i V_i = I_o V_o$$

$$[4,6] \quad (3)$$

and,

$$\frac{I_o}{I_i} = 1 - D \quad [4,6] \quad (4)$$

Where;

- $I_o$  : The average output current, Amp.
- $I_i$  : The average input current, Amp.

### 2-1-2 Discontinuons Conduction Mode

If the current following through the inductor falls to zero before the next turn-on of the switching IGBT's,

then the boost converter is said to be operating in the discontinuous conduction mode. If we equate the integral of the inductor voltage as shown in Fig. 2-4 over one time period to zero,

$$V_i D T_s + (V_i - V_o) D_1 T_s = 0 \quad [4,6] \quad (5)$$

Then;

$$\frac{V_o}{V_i} = \frac{D+D_1}{D} = \frac{1}{1-D_1} \quad [4,6] \quad (6)$$

and

$$\frac{I_o}{I_i} = \frac{D}{D+D_1} \quad (\text{since } P_i=P_o) \quad [4,6] \quad (7)$$

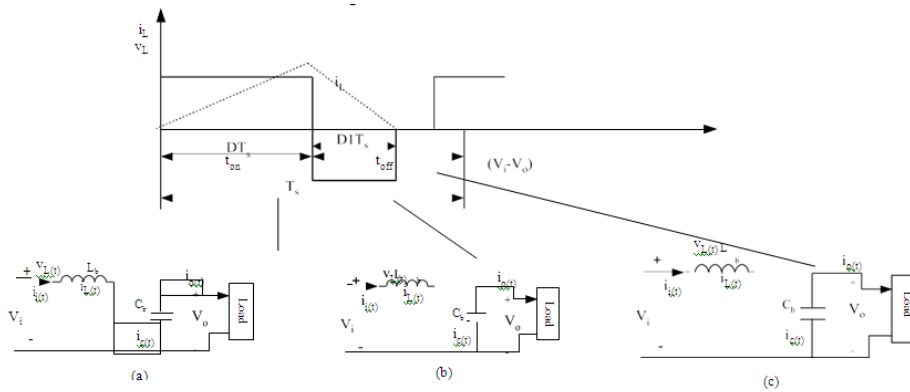


Fig. 3 Equivalent Circuit for boost Converter in DCM  
 (a) Mode 1 ( $0 < t \leq t_{on}$ ) (b) Mode 2 ( $t_{on} < t \leq (D+D1)T_s$ )  
 (c) Mode 3 ( $(D+D1)T_s < t \leq T_s$ )

From Fig. 3c, the average input current, which is equal to the inductor current, is

$$I_i = \frac{V_i}{\gamma T} \left[ \frac{D^2}{2} + D + 1 \right] \quad (8)$$

Using (Equ. (7)) in the foregoing equation yields

$$I_i = \frac{V_i}{\gamma T} \left[ \frac{D^2}{2} + D + 1 \right] \quad (9)$$

In practice, since  $V_o$  is held constant and  $D$  varies in response to variation in  $V_i$ , it is more useful to obtain the required duty cycle,  $D$ , as a function of load current for varies values of  $V_o/V_i$ . By using Eqns (6) and (9), we can determine that:

$$D = \left[ \frac{4 V_o}{27 V_i} \left( \frac{V_o}{V_i} - 1 \right) \frac{I_{o,aver,max}}{I} \right]^{0.5} \quad [4,6] \quad (10)$$

Where;

$I_{o,aver,max}$ : The maximum average output current at the edge of continuous conduction and can be found by the following Equation.

$$I_{o,aver} = \frac{T_s V_o}{2L_b} D(1-D)^2 \quad [4,6] \quad (11)$$

The average output current has its maximum at  $D=1/3$ .

$$I_{o,aver,max} = \frac{2 T_s V_o}{27 L_b} \quad [4,6] \quad (12)$$

The critical inductance,  $L_{bc}$ , is defined as the

inductance at the boundary edge between continuous and discontinuous modes and is defined as:

$$L_{bc} = \frac{R D (1-D)^2}{2 F_s} \quad [4,6] \quad (13)$$

where;

$R$  : The equivalent load,  $\Omega$ .

$F_s$  : The switching frequency, Hz

The switching frequency has been chosen arbitrarily to minimize the size of the boost inductor and limit the loss of the semiconductor device. At higher frequencies the switching losses in the IGBT's increase, and therefore reduce the overall efficiency of the circuit. At lower frequencies the required output capacitance and boost inductor size increases, and the volumetric efficiency of the supply degrades [9].

$V_{pv,max}$  : is the maximum input voltage from PV array, Volt.

The maximum current stress occurs when system power is predominantly provided by the PV. Therefore, the peak current is [9]

$$I_{peak} = I_{output} + I_{ripple} \quad (15)$$

$$I_{peak} = \frac{P_{in,max}}{V_{pv}} + \frac{\Delta I_{in,max}}{V_{pv}} \quad (16)$$

Where;

$P_{in,max}$  : Is the maximum output power from PV array which it is the input to boost converter.

$\Delta I$ : Is the percentage of ripple current to load output current.

### 2-3 Selection of the inductor

Large inductance values tend to increase the start-up time slightly while small inductance values allow the coil current to ramp up to higher levels before the switch turns off. Inductors with a ferrite core or equivalent are recommended. It should be ensured that the inductor's saturation current rating for highest efficiency is to be used a coil with low DC resistance. Boost inductance is selected based on the maximum allowed ripple current at minimum duty cycle,  $D$ , at maximum input voltage,  $V_{input}$ . Given that the switching frequency,  $F_s$ , the boost inductor value may be optimally determined to set the converter operating mode in the required load and line range. The critical inductance is defined as the inductance at the boundary edge between continuous and discontinuous modes and is defined as [4,6]:

$$L_c = \frac{R * D (1-D)^2}{2 * F_s} \quad (17)$$

Where,

$F_s$  : The switching frequency, Hz

$D$  : The duty cycle,

$R$  : The equivalent load,  $\Omega$ .

### 2-4 Selection of the Diode

The boost diode reverse voltage rating is limited to the output voltage. The diode conducts when the power switch is in the "OFF" state and provides a current path for the inductor to the output. Similar to the IGBT's the worst-case peak current through the diode occurs at low line input voltage and maximum load. Other important considerations in selecting the diode besides its ability to block the required off-state voltage stress and have sufficient peak and average current handling capability, is fast switching characteristics, low reverse-recovery, and low forward voltage drop.

**2-2 Selection Of The Semiconductor Device**

The main switching element has been chosen to handle the worst case current and voltage stresses. The maximum voltage stress on the switching device occurs when the PV output voltage is maximized, so:  
 $V_{max, stress} = V_{pv, max}$  (14)  
 Where;

**2-5 Selection of the capacitance required**

The primary criterion for selecting the output filter capacitor is its capacitance and equivalent series resistance, ESR. Since the capacitor's ESR affects efficiency, low-ESR capacitors will be used for best performance. For reducing ESR is also possible to connect few capacitors in parallel. The output filter capacitors are chosen to meet an output voltage ripple

specifications, as well as its ability to handle the required ripple current stress. An approximate expression for the required capacitance as a function of ripple voltage requirement,  $\Delta V_o$ , D, switching frequency,  $F_s$  and output voltage,  $V_o$  is given as [4,6]:

$$C_b \geq \frac{V_o * D}{F_s * \Delta V_o * R} \quad (18)$$

**III. APPLICATION AND RESULTS**

**3-1 Design DC/DC Boost converter**

A computer program has been designed to compute all inductances and capacitances for all duty cycle i.e for all radiations. To ensure DCM for these operating conditions the inductance have been chosen at a value smaller than the critical inductance and for this converter is set at 0.67 mH, 78  $\mu$ H and 22  $\mu$ H for variation of the load from 12kW, 200 kW and 500 kW respectively. Figures 4 & 5 show the value of critical inductance for critical conduction mode operation over the input voltage range i.e. for all radiation change. Figure 6 shows the relation between output capacitance and duty cycle. From this Figure it can be seen that required capacitance  $C_{req} \geq 3500\mu F$

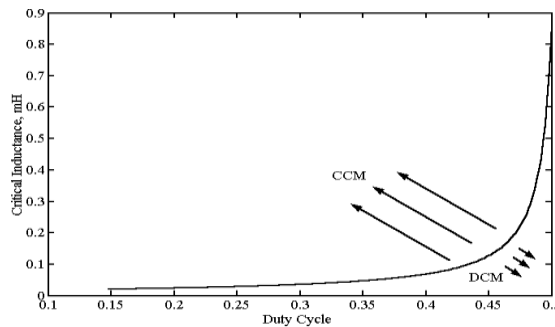


**Fig. 4** Relation Between Duty Cycle and Critical Inductance.

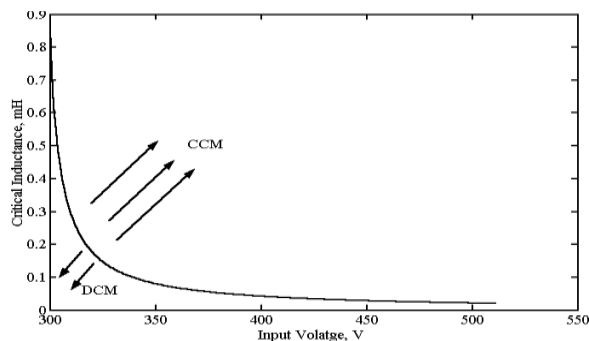


**Fig. 5** Relation Between Input Voltage and Critical Inductance.

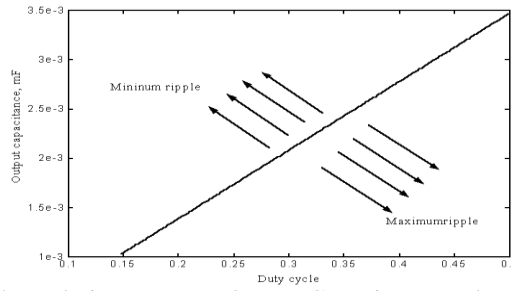


Fig. 6 The Relation Between Output Capacitance and Duty Cycle.

### 3.2 Simulation of DC/DC Converter

To verify the response of the converter as online algorithm, a complete dynamic model of PV array and DC/DC converter scheme have been simulated by Matlab/Simulink software [10],[11]. The DC/DC converter has been simulated for variation of the load from 12 kW, 200 kW and 500 kW respectively. The simulink block diagram of a boost converter and its controller is shown in Fig 7. The model's input is taken power from solar cells array and the output of the model is fed to the load demand. The output voltage from PV array,  $V_{dcpv}$  which is the input to boost converter is shown in Fig. 8. The PV array has been tested for load change due to change in solar radiation. The load set 12 kW at 9.30 A.M. for solar radiation 0.2 kWh/m<sup>2</sup>, 200 kW at 11.00 A.M. for solar radiation 0.6 kWh/m<sup>2</sup> and finally to 500 kW at 1.00 A.M. for solar radiation 1.0 kWh/m<sup>2</sup> and then back to 200 kW then 12 kW as shown in Fig. 9.

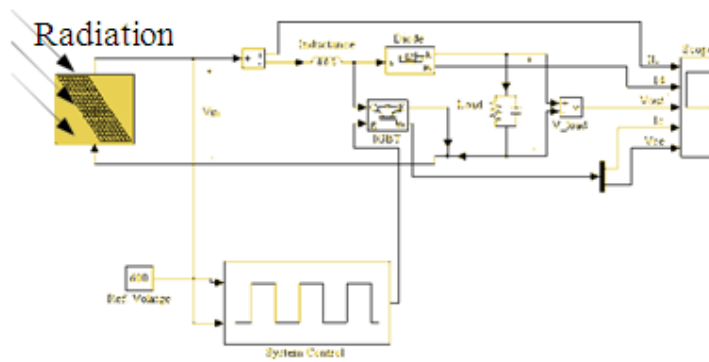


Fig. 7 Simulink Model for the Boost Converter with the Online Algorithm.

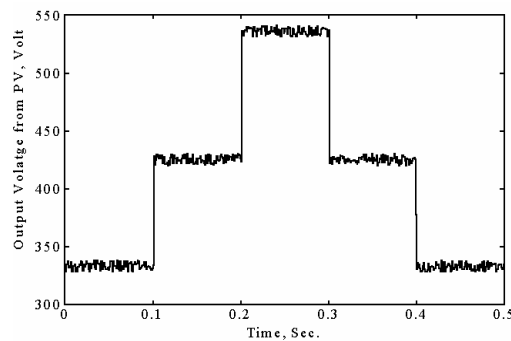
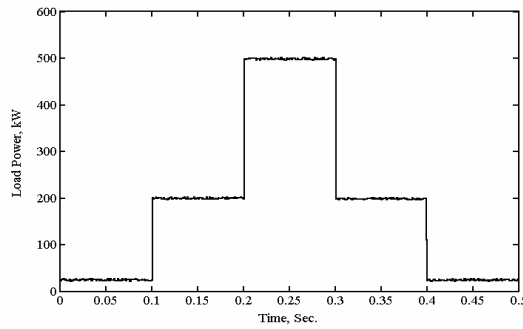
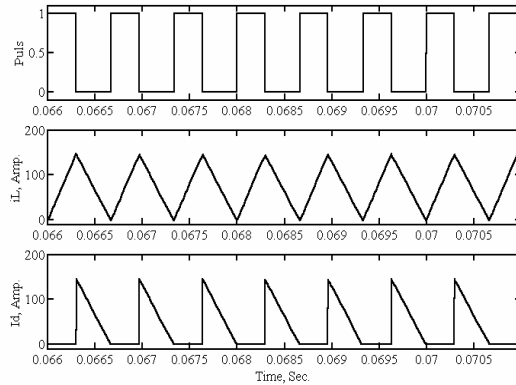


Fig. 8 Output Voltage from PV Solar Cells array due to Change of Radiation.



**Fig. 9** Load curve during the Day.

Simulations have been run at various loads to check the approximate boundary condition of the inductor and the soft switching of the devices. Once the simulation have been completed, the simulated response of diode's current and inductor's current for a radiation of  $0.2 \text{ kW/m}^2$  and load  $200 \text{ kW}$ , and  $1.0 \text{ kW/m}^2$  and load  $500 \text{ kW}$  are shown in Fig. 10 and Fig. 11. Also, Fig. 12, Fig. 13 and Fig. 14 show the input voltage and output voltage at a radiation of  $0.20 \text{ kW/m}^2$ ,  $0.6 \text{ kW/m}^2$  and  $1.0 \text{ kW/m}^2$  respectively. On the other hand Fig. 15, Fig. 16 and Fig. 17 show the IGBT's current,  $I_c$  and collector to emitter voltage,  $V_{ce}$  at a radiation of  $0.2 \text{ kW/m}^2$ ,  $0.6 \text{ kW/m}^2$  and  $1.0 \text{ kW/m}^2$  respectively.



**Fig. 10** Simulated Response of Diode's Current and Inductor's Current at Radiation of  $0.2 \text{ kW/m}^2$

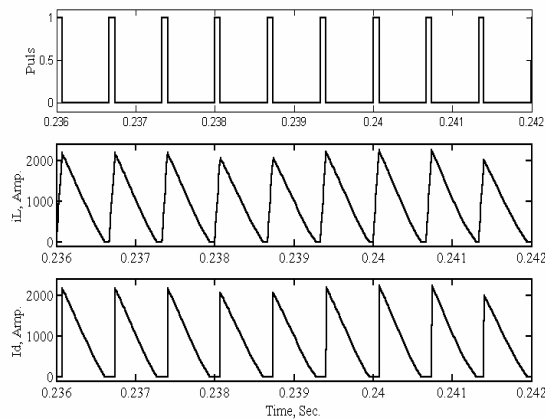


**Fig. 11** Simulated Response of Diode's Current and Inductor's Current at Radiation of  $1.0 \text{ kW/m}^2$

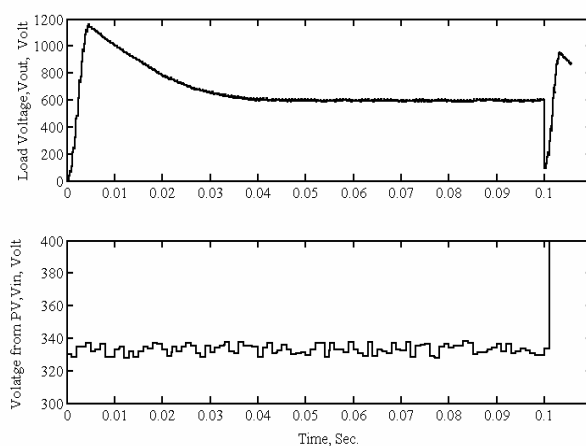


Fig. 12 Simulated Response of Input Voltage and Output Voltage at Radiation of 0.2 kw/m<sup>2</sup>

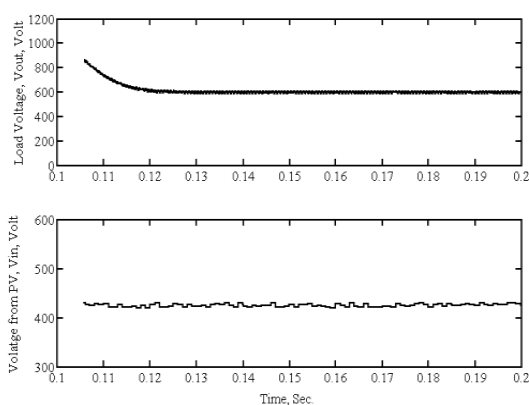


Fig. 13 Simulated Response of Input Voltage and Output Voltage at Radiation of 0.6 kw/m<sup>2</sup>

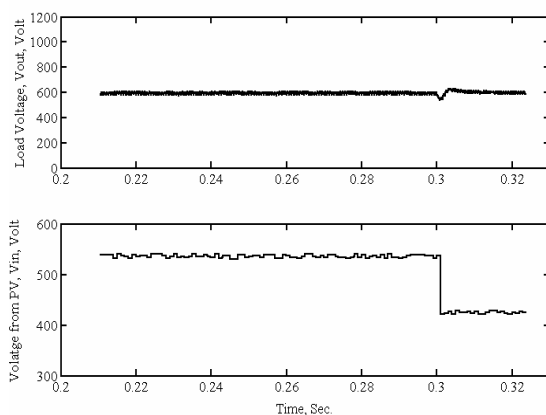
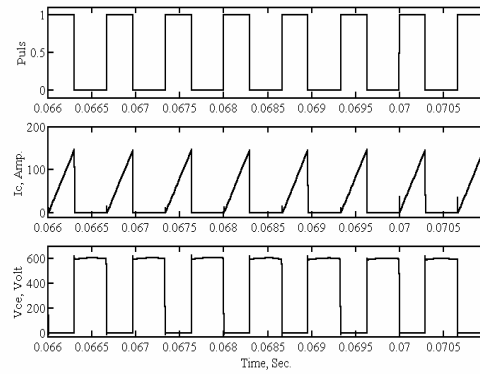
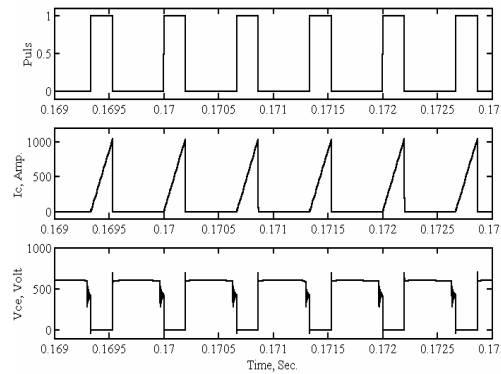


Fig. 14 Simulated Response of Input Voltage and Output Voltage at Radiation of 1.00 kw/m<sup>2</sup>



**Fig. 15** Simulated Response of IGBT's Current and Collector-Emitter Voltage at Radiation of 0.2 kw/m<sup>2</sup>



**Fig. 16** Simulated Response of IGBT 's Current and Collector-Emitter Voltage at Radiation of .6 kw/m<sup>2</sup>

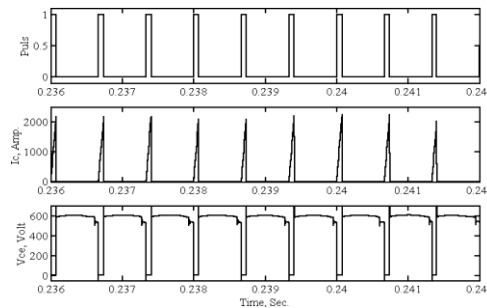


**Fig. 17** Simulated Response of IGBT 's Current and Collector-Emitter Voltage at Radiation of 1.0 kw/m<sup>2</sup>

The simulated response of output voltage is displayed in Fig. 18 for all radiation condition during the day. On the other hand, the simulated inductor current, diode current and IGBT's current for all periods i.e. for all variation of radiation during the day are shown in Fig. 19, Fig. 20 and Fig. 21 respectively. Finally, from all the above figures, overall converter works well. The output voltage variation can be resolved with the inverter control strategy.

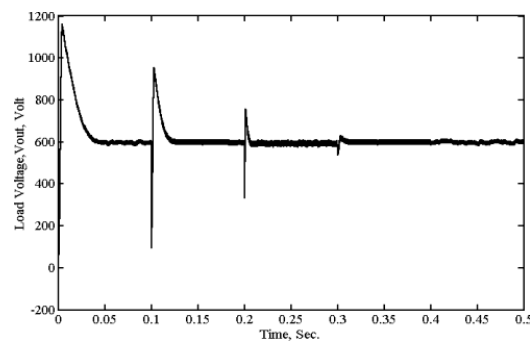


**Fig. 18** Simulated Response of Output Voltage due to change of Radiation during the Day



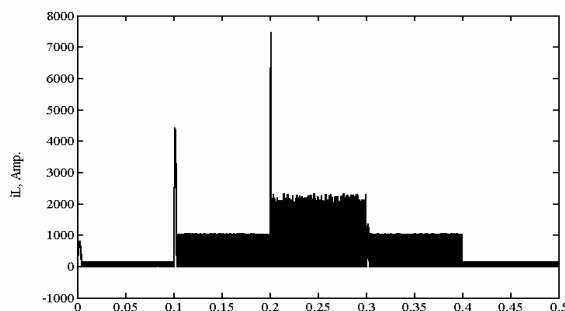


Fig. 19 Simulated Response of Inductor Current due to change of Radiation for all Day

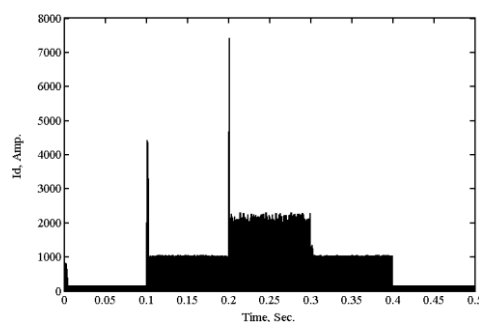


Fig. 20 Simulated Response of Diode Current due to change of Radiation during the Day

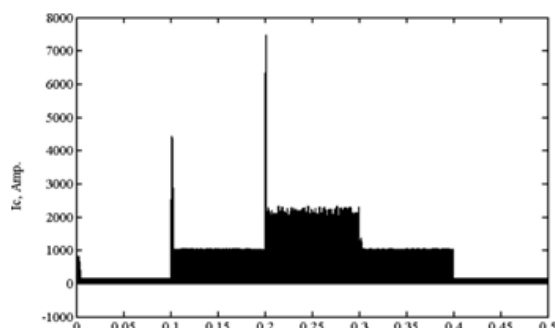


Fig. 21 Simulated Response of IGBT's Current due to change of Radiation during the Day

#### IV. CONCLUSION

This paper concerns with design and simulation of DC/DC boost converter to operate in PV system. From the results obtained above, the following are the salient conclusions that can be drawn from this paper:

- Design the DC/DC converter for all operating condition have studied and proposed.
- Detailed modeling and simulation of a DC/DC converter connected to PV system have proposed.
- Boost inductor is chosen to be 0.67 mH, 78 $\mu$ H and 22 $\mu$ H for variation of the load from 12kW to 500kW.
- Boost capacitance is chosen to be greater than or equal 3500 $\mu$ F for variation of the load from 12kW to 500kW.

#### REFERENCES

- [1]. Konstantin P. Louganski, "Modeling and Analysis of A DC Power Distribution System In 21<sup>st</sup> Century Airlifters", M. Sc., Electrical Engineering Dept., Faculty of the Virginia Polytechnic Institute and State University, September 30, 1999, Blacksburg, Virginia.
- [2]. Jaber Abu-Qahouq and Issa Batarseh, "Generalized Analysis of Soft-Switching DC-DC Converters", ISCAS 2000 - IEEE International Symposium on Circuits and Systems, May 28- 31, 2000, Geneva, Switzerland, pp.507-510.
- [3]. Woywode, O.; Guldner, H. "Application of Statistical Analysis to DC-DC Converter" International Power Electronics Conference, IPEC 2000, Tokyo, Japan 2000.
- [4]. Mohammad H. Rashid, "Power Electronics: Circuits, Devices and Applications", Prentice-Hall, Inc., Englewood Cliffs, Book, Second Edition, 1993.
- [5]. B. W. Williams, " Power Electronics; Devices, Drivers, Applications and Passive Components", Book, Second Edition, Educational Low-Priced Books Scheme; ELBS, 1992.
- [6]. Mohan Ned, Undeland Tore M. and Robbins William P. Power Electronics ,Converters Applications and Design", John Wiley & Sons, Inc., Book, 1995.
- [7]. C. K. Tse and K. M. Adams, "Qualitative analysis and control of a DC-to-DC Boost Converter Operating in Discontinuous Mode",

- IEEE Transactions on Power Electronics, Vol. 5, No. 3, July 1999, Pp 323-330.
- [8]. Adel A. Elbaset Mohammed, " Study of Interconnecting Issues of Photovoltaic/Wind Hybrid System with Electric Utility Using Artificial Intelligence ", Ph. D. Thesis, Faculty of Eng., Electrical Engineering Dept., Minia University , 2006.
- [9]. <http://onsemi.com/AND8035-D.pdf>
- [10]. Matlab-Simulink User's Guide", Themathworks, Version 6.0.0.88 R12.
- [11]. Power System Blockset User's Guide", The Mathworks, Version 6.0.0.88 R12.